PNAS RESEARCH ARTICLE | ENVIRONMENTAL SCIENCES ECOLOGY

Leaf hydraulic and photosynthetic traits mediate forest-scale resource use efficiencies across the continental United States

Bailu Zhao[a], Lawren Sack[b], Hannes Paul T. De Deurwaerder[a,c], Camila D. Medeiros[b,d], Nidhi Vinod[b], Marvin Browne[e], Jeffrey D. Wood[f], K. C. Cushman[g], Elena Shevliakova[h], Sergey Malyshev[h], Anna Jiselle Ongjoco[b], Anna Trugman[i], David A. Orwig[j], Christina McKeown[k], Joseph Zailaa[l], Daniel J. Johnson[m], Lukas Magee[m,n], Sean McMahon[o,p], Jess Shue[o], Karina Schafer[q], Sean Burns[r,s], Peter D. Blanken[r], and Matteo Detto[a,t,1]

Affiliations are included on p. 9.

Edited by William H. Schlesinger, Cary Institute of Ecosystem Studies, Millbrook, NY; received October 6, 2025; accepted September 24, 2026

Temperate forests play a critical role in global carbon cycling and other ecosystem services, yet their resilience to climatic stresses remains uncertain. We combined physiology, community composition, flux data, and modeling to test a functional trait-based approach to predict forest ecosystem processes. For eight U.S. forests spanning broad precipitation and temperature gradients, we scaled up key leaf functional traits—maximum carboxylation velocity of Rubisco ($V_{c,max}$), maximum leaf hydraulic conductance ($K_{l,max}$), and turgor loss point (that is, wilting point, π_{tlp}) to predict gross primary productivity, light-use efficiency, standard and intrinsic water-use efficiency (WUE and iWUE), and their sensitivities to soil drought. In multiple regressions, ecosystem processes were strongly associated with community-weighted mean (CWM) trait values: enhanced productivity was linked with high $\overline{V_{c,max}}$, $\overline{K_{l,max}}$ and $\overline{\pi_{tlp}}$, whereas high WUE and iWUE were linked with low $\overline{K_{l,max}}$ and high $\overline{\pi_{tlp}}$. The CWM functional traits also influenced the sensitivity of ecosystem processes to soil moisture. A causal role of functional traits in driving ecosystem processes alongside climate was supported by parameterizing the LM4.1 vegetation model with CWM functional traits. This study highlights the important role of functional traits in determining forest responses to climate-driven water stress at a continental scale.

functional traits | continental gradients | climate | ecosystem processes | soil water content

Significance

This study investigates the role of leaf functional traits in driving forest processes across a continental-scale climatic gradient. For eight temperate forests, ecosystem productivity and water use efficiency, and their sensitivity to drought, are linked with community weighted mean photosynthetic and hydraulic traits. The patterns were captured by an ecosystem model parameterized with observed trait variation that mechanistically links forest productivity to leaf functional traits. As climate change leads to intensified droughts, functional traits can enable mechanistic predictions of forest resilience and carbon storage capacity.

To predict and manage the future of our biosphere, there is an increasingly urgent need to understand the underlying drivers of ecosystem processes. Shifts in drought frequency and intensity threaten the ability of forests to assimilate carbon, increase their carbon losses through tree mortality, and disrupt ecosystem services such as fostering biodiversity and healthy biogeochemical cycles (1–3). Temperate forests account for 14% of global forest carbon storage (4). Addressing the challenge of clarifying and predicting their responses to climate variation requires the integration of approaches at multiple scales across continental gradients (5).

At large scales, ecosystem responses to drought and other environmental stressors are often evaluated by considering ecosystem processes, in particular the gross primary productivity (GPP) and its magnitude relative to resource availability, that is, resource-use efficiencies (RUEs), including light-use efficiency (LUE) and standard and intrinsic water-use efficiencies (WUE and iWUE, respectively) (6–9). Ecosystem RUEs vary strongly among communities and along climatic and edaphic gradients (10, 11). Yet, the mechanisms for this variation at continental scales remain unclear. As variation among sites with similar macroclimate can be enormous, climatic factors alone cannot fully account for shifts in ecosystem responses to environmental variation (9). Thus, novel tests of other potential drivers of ecosystem RUEs—most notably plant functional traits—are needed (12). Plant functional traits are characteristics that influence plant growth, reproduction, and survival, and thereby fitness (13, 14), and their inclusion has informed many approaches in organism- and community-scale ecology for decades (15). Species' traits are shaped by long-term climatic conditions that optimize resource use and enhance resilience to environmental stresses and disturbances (13), but also by biotic interactions such as interspecific competition (16). Recent studies comparing global eddy flux tower sites showed that ecosystem processes were correlated with species averages across sites for several compositional and structural traits, e.g., foliar nitrogen concentration, maximum leaf area index, and maximum canopy height (9). However, the quantitative influence of leaf hydraulic and photosynthetic traits on ecosystem processes across gradients has not been tested, owing to the lack of data for community weighted

Author contributions: B.Z., L.S., A.T., and M.D. designed research; B.Z. and M.D. performed research; E.S. and S. Malyshev contributed new reagents/analytic tools; B.Z. and M.D. analyzed data; L.S., H.P.T.D.D., C.D.M., N.V., M.B., J.D.W., A.J.O., D.A.O., C.M., J.Z., D.J.J., S. McMahon, J.S., K.S., S.B., P.D.B., and M.D. collected data; H.P.T.D.D., K.C.C., and K.S. revised the manuscript; and B.Z., L.S., and M.D. wrote the paper.

The authors declare no competing interest.

This article is a PNAS Direct Submission.

Copyright © 2026 the Author(s). Published by PNAS. This article is distributed under Creative Commons Attribution-NonCommercial-NoDerivatives License 4.0 (CC BY-NC-ND).

[1]To whom correspondence may be addressed. Email: mdetto@princeton.edu.

This article contains supporting information online at https://www.pnas.org/lookup/suppl/doi:10.1073/pnas.2526434123/-/DCSupplemental.

Published November 9, 2026.

Downloaded from https://www.pnas.org by HARVARD UNIVERSITY; CABOT SCIENCE LIBRARY on November 19, 2026 from IP address 140.247.220.94.

mean (CWM) traits at flux sites (17). This is primarily because plant trait measurements obtained through standardized methods, species-abundance data, and coordinated flux observations are rarely available within the same sites.

Leaf-scale traits such as maximum carboxylation velocity ($V_{c,max}$), maximum leaf hydraulic conductance ($K_{l,max}$), and turgor loss point (π_{tlp}) play direct, pivotal roles in plant function by influencing photosynthesis and transpiration, and are thus prime candidates for traits that would scale up from plant physiology to ecosystem processes (18). $V_{c,max}$ reflects the optimization of carbon assimilation to temperature, light, and nutrient availability, and thus a higher $V_{c,max}$ potentially enhances GPP, LUE, WUE, and iWUE across a range of resource availability and stress conditions (19). Similarly, $K_{l,max}$ represents the efficiency of water transport through the leaf [i.e., the flow rate for a given water potential driving force (20)], and enables high stomatal conductance and light-saturated photosynthetic rates across diverse species and within lineages (21–24). Therefore, a higher $K_{l,max}$ would, in principle, contribute to a higher GPP, while sustaining a high stomatal conductance that would reduce WUE and iWUE. Whereas these traits are primarily linked to productivity, a low π_{tlp} enhances drought tolerance by keeping stomata open and sustaining photosynthesis at lower water potentials (25). Yet, across diverse species, a high π_{tlp} may be linked with greater stomatal conductance under high moisture availability (26). Thus, at the ecosystem scale, a high π_{tlp} may be a driver of high GPP, WUE, and iWUE (27). Notably, trade-offs described at plant scale have linked high $K_{l,max}$ and π_{tlp} with sharper declines in hydraulic and stomatal conductance during dehydration (26, 28), and these effects would be expected to influence ecosystem processes under drought. Importantly, given that traits vary widely across species even within the same community (20, 29), CWM functional trait values, rather than unweighted community species averages or the trait values of single species, would be expected to predict forest-scale functions and their responses to climate.

We conducted a critical test of the influence of these plant functional traits on ecosystem processes across forests at the continental scale. For eight temperate forests across the United States, diverse in structure, species composition, and function (Fig. 1), we measured community biomass-weighted means for $V_{c,max}$, $K_{l,max}$, and π_{tlp} (hereafter referred to as $\overline{V_{c,max}}$, $\overline{K_{l,max}}$ and $\overline{\pi_{tlp}}$). Using both flux tower datasets and the Land Component (Land Model Version 4.1, or LM4.1) of the Geophysical Fluid Dynamics Laboratory (GFDL) Earth System Model Version 4.1 (ESM4.1), we analyzed the control of plant functional traits and environmental forcing on ecosystem processes.

Previous studies have incorporated plant functional traits into analyses of ecosystem responses to environmental stressors, and found these to greatly improve process-based models for predicting

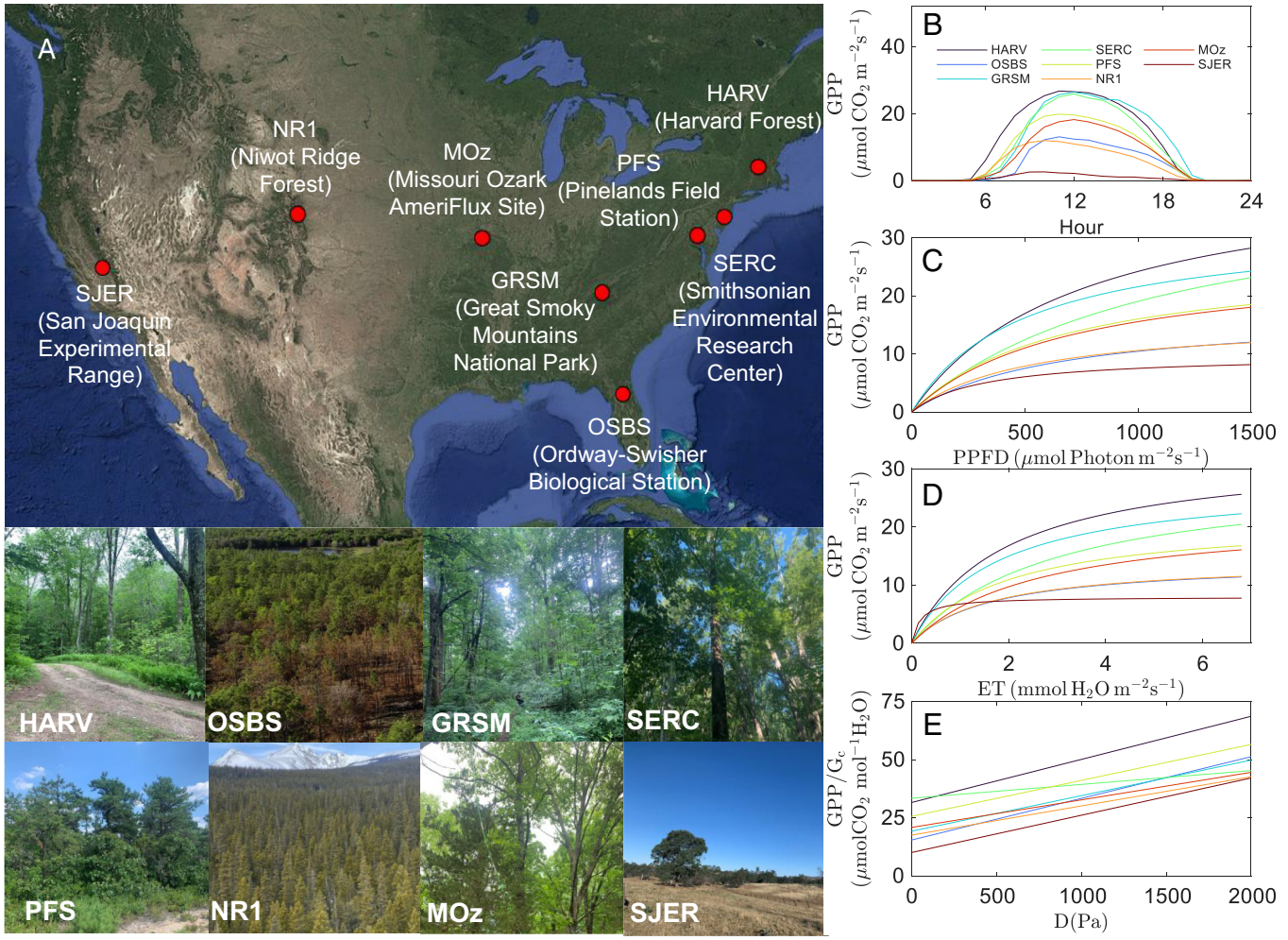


Fig. 1. Studied forests across the continental USA with diverse ecosystem functions: (*A*) map and site images of each site, (*B*) diurnal gross primary productivity (GPP) during the growing season, and response curves of GPP to (*C*) irradiance, quantified as photosynthetic photon flux density (*I*), (*D*) evapotranspiration rate (ET) and (*E*) vapor pressure deficit (D) for each site. For more details on site information, see Table 1.

Downloaded from https://www.pnas.org by HARVARD UNIVERSITY; CABOT SCIENCE LIBRARY on November 19, 2026 from IP address 140.247.220.94.

Table 1. Forest study sites across the continental USA

Site name	HARV	OSBS	GRSM	SERC	PFS	NR1	MOz	SJER
Site description	Harvard Forest	Ordway-Swisher Biological Station	Great Smoky Mountains National Park	Smithsonian Environmental Research Center	Pinelands Field Station	Niwot Ridge Forest	Missouri Ozark AmeriFlux Site	San Joaquin Experimental Range
AmeriFlux site code	US-Ha1	US-xSB	US-xGR	US-xSE	US-Slt	US-NR1	US-MOz	US-xSJ
LAT (°N)	42.5	29.7	35.7	38.9	39.9	40	38.7	37.1
LON (°E)	−72.2	−82	−83.5	−76.6	−74.6	−105.5	−92.2	−119.7
ELE(m)	340	45	579	15	30	3050	219	368
GST (°C)	11.5	23	17.4	18.9	16	5.9	17.5	18.7
GSP (mm/d)	3.6	4	3.7	3.8	3.3	1.8	2.6	2.3
GSAI	0.62	0.44	0.41	0.43	0.49	0.26	0.31	0.21
Forest type	Broadleaf-Deciduous	Conifer-Evergreen	Broadleaf-Deciduous	Broadleaf-Deciduous	Conifer-Evergreen	Conifer-Evergreen	Broadleaf-Deciduous	Broadleaf-Deciduous
LAI	4.8	1.4	4.2	4.8	4.3	2.2	5	1.8
Canopy height (m)	24	23	40	38	18	13	22	21
Flux tower measurement period	2009–020	2020–2021	2020–2022	2020–2022	2009–2014	2002–2022	2004–2021	2019–2021

Abbreviations: latitude (LAT), longitude (LON), elevation (ELE), growing season temperature, precipitation, and aridity index (GST, GSP, and GSAI, respectively, where GSAI is calculated from flux tower data as GSP divided by growing season potential evapotranspiration from the Penman equation, leaf area index (LAI, the one-sided value for the peak growing season retrieved from MODIS dataset), and canopy height retrieved from flux tower metadata and site description pages, NEON site description pages, LiDAR product (30), and the literature (31–33).

Downloaded from https://www.pnas.org by HARVARD UNIVERSITY; CABOT SCIENCE LIBRARY on November 19, 2026 from IP address 140.247.220.94.

climate change impacts for individual sites (34–36). Our study tests the hypothesis that plant functional traits mediate ecosystem processes at the continental scale. This test was enabled by three methodological innovations designed to achieve high resolution. First, our study focused on directly mechanistic traits (e.g., $V_{c,max}$, $K_{l,max}$, and π_{tlp}), rather than easier-to-measure proxy traits such as leaf mass per area and nitrogen content per unit of mass (also measured but not analyzed here). $V_{c,max}$ is a focus of global studies on GPP drivers and is among the most important parameters in Earth System Models (37). Recent advancements in these models have included the role of plant hydraulics in regulating stomatal behavior and photosynthesis (38–41). Because leaf hydraulics often constitute a bottleneck in the whole-plant water transport pathway (42), we focus here on $K_{l,max}$ and π_{tlp}. Second, we made in situ measurements of these functional traits for the biomass-dominant species in each forest, an approach that more directly assesses the controls of functional traits and environmental forcing on ecosystem processes than the use of databases compiled from plants in different locations using different methods (43), or relying on fixed, averaged functional trait values assigned to plant functional types (PFTs) (44). Third, we extended prior work that examined the influence of plant functional traits on ecosystem processes at individual sites (45), along elevational transects (46), or in nonforest ecosystems (47), by instead considering diverse temperate forests across a continental gradient. Understanding how plant functional traits regulate ecosystem processes at the continental scale is important for trait-based predictions of carbon budgets and land–atmosphere interactions under changing climates and shifting species distributions (5).

We tested three hypotheses related to the influence of plant functional traits on key ecosystem processes at a continental scale. First, we hypothesized that functional traits would have control over ecosystem processes comparable to or stronger than that of climate and soil nitrogen concentration. Second, we hypothesized that ecosystems with relatively acquisitive functional traits (high $\overline{V_{c,max}}$, $\overline{K_{l,max}}$, and $\overline{\pi_{tlp}}$) maximize photosynthesis, leading to higher light-saturated GPP and LUE, and that high $\overline{V_{c,max}}$, high $\overline{\pi_{tlp}}$, and low $\overline{K_{l,max}}$ would confer higher iWUE and WUE. Finally, we hypothesized that ecosystems with acquisitive functional traits would show steeper reductions in LUE, and greater increases in WUE and iWUE under declining soil moisture.

Results

Influence of Plant Functional Traits on Ecosystem Processes Across a Continental Gradient. Across the eight forests, CWM values of plant functional traits were important statistical drivers of productivity and resource use efficiencies (RUEs; R^2 of overall models predicting ecosystem process parameters from plant functional traits = 0.1 to 0.72; Fig. 2). Ecosystem maximum productivity given saturating light ($P_{L,max}$) and given full hydration ($P_{W,max}$) were both positively associated with $\overline{V_{c,max}}$ and $\overline{\pi_{tlp}}$ ($P < 0.01$, Fig. 2; see Table 2 for definitions of ecosystem process parameters). These relationships held when considering ecosystem maximum productivity on a leaf area basis, i.e., normalizing by leaf area index (LAI): $P^*_{L,max}$ and $P^*_{W,max}$ were positively associated with $\overline{\pi_{tlp}}$ ($P < 0.05$). Additionally, the half-saturation points of light and water use ($I_{L,0}$ and $I_{W,0}$), which are metrics of light and water-use efficiency (Table 2), were positively associated with $\overline{V_{c,max}}$ and $\overline{\pi_{tlp}}$ ($P < 0.05$). Further, the intrinsic water use efficiency at the site-specific median vapor pressure deficit ($iWUE_{\bar{D}}$) was positively associated with $\overline{V_{c,max}}$ and negatively with $\overline{K_{l,max}}$ ($P < 0.01$). These results overall indicate a strong ability of these functional traits to predict ecosystem processes across a continental gradient. By contrast, ecosystem processes were statistically uncoupled from other functional traits: $P^*_{L,max}$ and $P^*_{W,max}$ from $\overline{V_{c,max}}$ and $\overline{K_{l,max}}$, LUE and WUE parameters from $\overline{K_{l,max}}$, and $iWUE_{\bar{D}}$ from $\overline{\pi_{tlp}}$.

We also found evidence supporting the influence of $\overline{V_{c,max}}$ on the response of ecosystem processes to soil water content (SWC). Across the forests, the sensitivity of $P_{L,max}$ to SWC was positively associated with higher $\overline{V_{c,max}}$ ($P < 0.05$), and other ecosystem

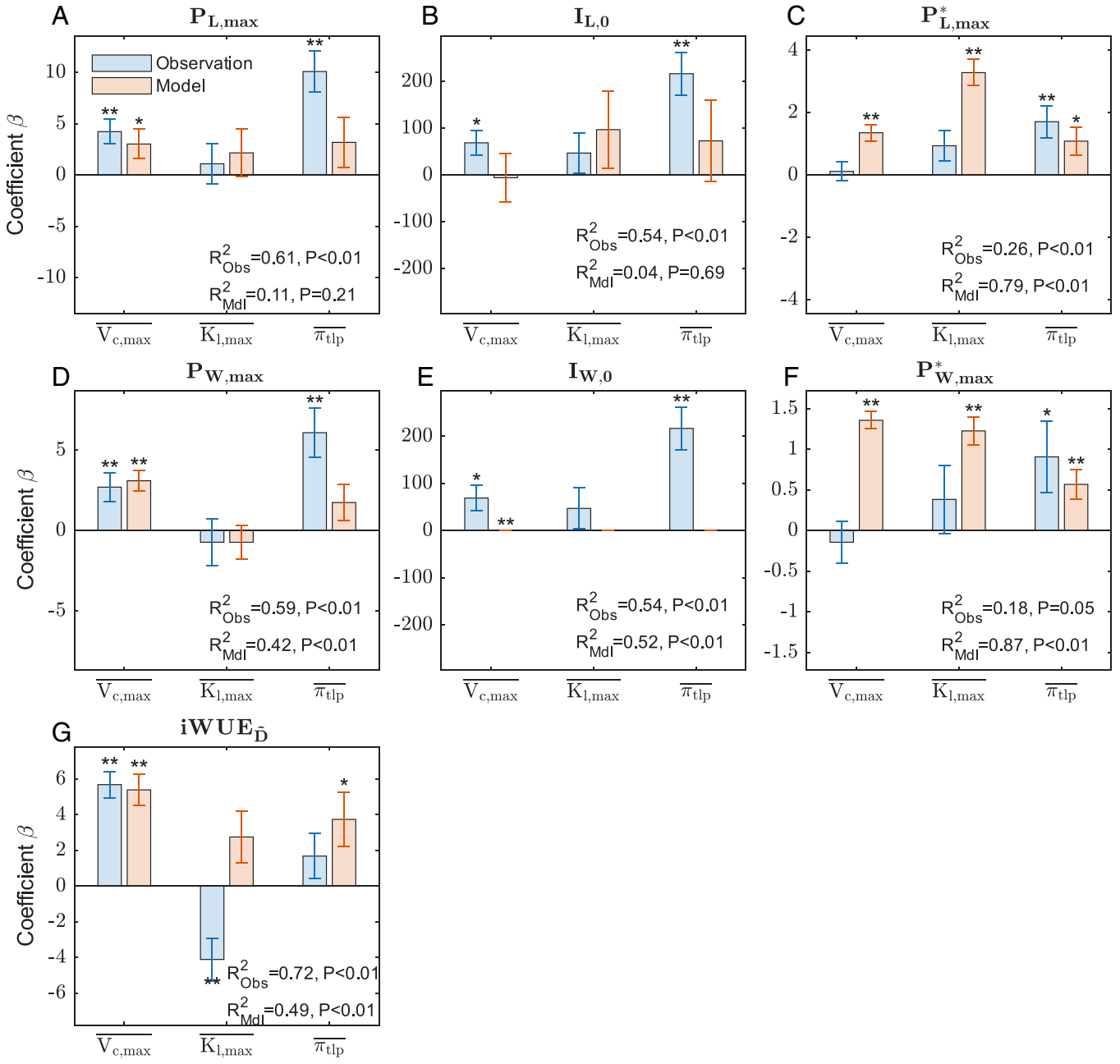


Fig. 2. The control of plant traits on ecosystem process parameters: light use efficiency (LUE, top row, *A–C*), water use efficiency (WUE, middle row, *D–F*), and intrinsic water use efficiency ($iWUE_{\tilde{D}}$, bottom row, *G*). $P_{L,max}$ and $P_{W,max}$ are the maximum GPP given saturating light and full hydration, respectively; $I_{L,0}$ and $I_{W,0}$ are the half-saturation points of light and water use, respectively; $P^*_{L,max}$ and $P^*_{W,max}$ are $P_{L,max}$ and $P_{W,max}$ per unit leaf area. $iWUE_{\tilde{D}}$ is intrinsic water use efficiency at site-specific median water pressure deficit. $\overline{V_{c,max}}$, $\overline{K_{l,max}}$ and $\overline{\pi_{tlp}}$ are community biomass-weighted means for maximum carboxylation velocity ($V_{c,max}$), maximum hydraulic conductance ($K_{l,max}$), and turgor loss point (π_{tlp}). The stars indicate the *t*-statistical significance of coefficient β, the whiskers are the SE of estimations (Eq. **4**), $^*P < 0.05$ and $^{**}P < 0.01$).

process parameters showed positive empirical trends (*SI Appendix*, Fig. S11).

Influence of Climate Forcing on Ecosystem Processes Across a Continental Gradient. The power of traits to predict ecosystem productivity and RUEs across the eight forests was comparable to that of site-level mean environmental variables (R^2 = 0.20 to 0.84). Maximum productivity ($P_{L,max}$, $P_{W,max}$, $P^*_{L,max}$ and $P^*_{W,max}$), half-saturation points ($I_{L,0}$ and $I_{W,0}$), and intrinsic water use efficiency ($iWUE_{\tilde{D}}$) were all positively associated with the growing-season aridity index (GSAI, for which higher values correspond to greater climatic moisture) ($P < 0.05$). Additionally, $I_{L,0}$ and $I_{W,0}$ were negatively associated with soil nitrogen concentration ($P < 0.01$, Fig. 3). By contrast, growing-season temperature (GST) was not a significant statistical driver of any ecosystem processes. Site-level mean environmental variables did not predict the responses of ecosystem processes to SWC (*SI Appendix*, *Text S1*).

Notably, climate forcing variables and CWM traits exhibited several intercorrelations. Most notably, $\overline{V_{c,max}}$ was positively correlated with GST, and to a lesser extent with GSP and GSAI. $\overline{K_{l,max}}$ was weakly negatively correlated with GSP and GSAI, whereas $\overline{\pi_{tlp}}$ was positively correlated with GSP and GSAI (*SI Appendix*, Fig. S12). We tested the relative importance of CWM traits and climate forcing variables in explaining ecosystem process parameters by fitting linear models based on the six factors and hierarchical partitioning their relative contributions of R^2. We found that, across the seven ecosystem process parameters, the

Downloaded from https://www.pnas.org by HARVARD UNIVERSITY; CABOT SCIENCE LIBRARY on November 19, 2026 from IP address 140.247.220.94.

Table 2. Equations for ecosystem processes and summary of ecosystem process parameters

Ecosystem process	Ecosystem resource use efficiency	Fitting curve	Process parameters	Unit of parameters	Physical meaning of parameters
Light response	Light-use efficiency $LUE = \frac{GPP}{I}$	$GPP = \frac{P_{L,max}}{I_{L,0}+I}$	$P_{L,max}$	μmol C m^{-2} s^{-1}	Maximum GPP at saturating irradiance
			$I_{L,0}$	μmol Photon m^{-2} s^{-1}	Irradiance at which GPP reaches its half-maximum; a lower value indicates a steeper light response
			$P^*_{L,max} = \frac{P_{L,max}}{LAI}$	μmol C m^{-2} s^{-1}	Maximum GPP at saturating irradiance per unit leaf area
Moisture response	Standard water use efficiency $WUE = \frac{GPP}{ET}$	$GPP = \frac{P_{W,max}}{I_{W,0}+ET}$	$P_{W,max}$	μmolC m^{-2} s^{-1}	Maximum GPP at high water consumption
			$I_{W,0}$	μmolC $mol^{-1}H_2O$	Water consumption when GPP reaches its half-maximum; a lower value indicates a steeper moisture response
			$P^*_{W,max} = \frac{P_{W,max}}{LAI}$	μmolC m^{-2} s^{-1}	Maximum GPP at high water consumption per unit leaf area
	Intrinsic water use efficiency $iWUE = \frac{GPP}{G_c}$	$\frac{GPP}{G_c} = a + bD$	$iWUE_{\tilde{D}}$	μmolC $mol^{-1}H_2O$	GPP per unit of canopy conductance at site-specific median vapor pressure deficit ($\tilde{D}$)

three CWM traits jointly explained 25 to 48% of R^2, comparable to the 31 to 54% explained by the three climate variables (*SI Appendix*, Fig. S13).

Validation of Plant Functional Traits and Climate Forcing Controls Over Ecosystem Processes Using LM4.1. For each forest, we ran ecosystem model LM4.1 with CWM plant functional trait values as model parameters, in conjunction with calibration of other key parameters, including the stomatal sensitivity parameter m of the Leuning stomatal conductance model and the dark respiration parameter (γ_{res}; for definition, see *SI Appendix, Text S2* and Eq. **S1b**). Simulations were driven by site-specific climate forcings. Compared with simulations driven by the default LM4.1 parameters, implementing measured CWM functional trait values improved the accuracy of the model (*SI Appendix, Text S3*). We validated the mechanistic influence of functional traits and forcing on ecosystem processes using LM4.1 in two ways. First, we quantified the sensitivity of the modeled ecosystem processes to each individual functional trait. Second, we analyzed the model-predicted ecosystem processes using the same linear equations as for the observed data (see previous sections of *Results*), to determine the statistical associations with functional traits and forcing.

The sensitivity analysis of the model supported the strong mechanistic influence of the CWM functional traits on ecosystem processes across the eight forests (*SI Appendix, Text S4*). Considering median values calculated across the forests, all ecosystem process parameters ($P_{L,max}$, $P_{W,max}$, $I_{L,0}$ and $I_{W,0}$) increased with higher $\overline{V_{c,max}}$, $\overline{K_{l,max}}$ and $\overline{\pi_{tlp}}$ (*SI Appendix*, Table S3), except for $iWUE_{\tilde{D}}$, which increased with higher $\overline{V_{c,max}}$ and $\overline{\pi_{tlp}}$, and decreased with higher $\overline{K_{l,max}}$.

The statistical effects of CWM functional traits on ecosystem process parameters were generally consistent between the LM4.1 model simulations and observations (Fig. 2). The model reproduced the significant control of maximum productivity by CWM functional traits: $P_{L,max}$ and $P_{W,max}$ were positively associated with $\overline{V_{c,max}}$, $P^*_{L,max}$ and $P^*_{W,max}$ with $\overline{\pi_{tlp}}$, and $P^*_{L,max}$ with $\overline{K_{l,max}}$ (R^2 = 0.11-0.87; $P < 0.05$). Further, consistent with observations, modeled $I_{W,0}$ and $iWUE_{\tilde{D}}$ were positively associated with $\overline{V_{c,max}}$ ($P < 0.05$). Yet, certain ecosystem process parameters based on model simulations showed associations with CWM functional traits that were not found in the observed data. For example, analysis of model simulations showed a negative association of $iWUE_{\tilde{D}}$ with $\overline{K_{l,max}}$ (R^2 = 0.49; $P < 0.01$). Several key statistical effects of climate drivers on ecosystem process parameters were also consistent between the LM4.1 model simulations and observations. Specifically, model simulations also found significant control of GSAI over maximum productivity ($P_{L,max}$ and $P_{W,max}$), half-saturation points ($I_{L,0}$ and $I_{W,0}$), and $iWUE_{\tilde{D}}$ (R^2 = 0.44 to 0.75; $P < 0.01$; Fig. 3). Notably, several ecosystem process parameters based on model simulations showed associations with climate drivers that were not found in the analyses of observed data. For example, analyses of the model simulations showed a negative control of GST over $P_{L,max}$, $P_{W,max}$, $I_{L,0}$ and $I_{W,0}$ ($P < 0.01$). The model also showed positive control of soil N over $I_{L,0}$ ($P < 0.01$), where observations suggested a negative control. For the model simulations, across the seven ecosystem process parameters, the three CWM traits jointly explained 6 to 79% of R^2, comparable to the 14 to 58% explained by the three climate variables (*SI Appendix*, Fig. S13).

In the model simulations, we found the sensitivity of ecosystem process parameters to SWC was associated with CWM traits and climate variables. These associations were not detected in the observed data. For example, the response of $P_{L,max}$ to SWC was negatively related to $\overline{K_{l,max}}$ and positively related to $\overline{\pi_{tlp}}$, and the response of $P^*_{W,max}$ to SWC was significantly positively related to $\overline{K_{l,max}}$ (*SI Appendix*, Fig. S11). The modeled responses of $P^*_{L,max}$ and $P^*_{W,max}$ to SWC were positively related to GSAI ($P < 0.05$; *SI Appendix, Text S1*).

Downloaded from https://www.pnas.org by HARVARD UNIVERSITY; CABOT SCIENCE LIBRARY on November 19, 2026 from IP address 140.247.220.94.

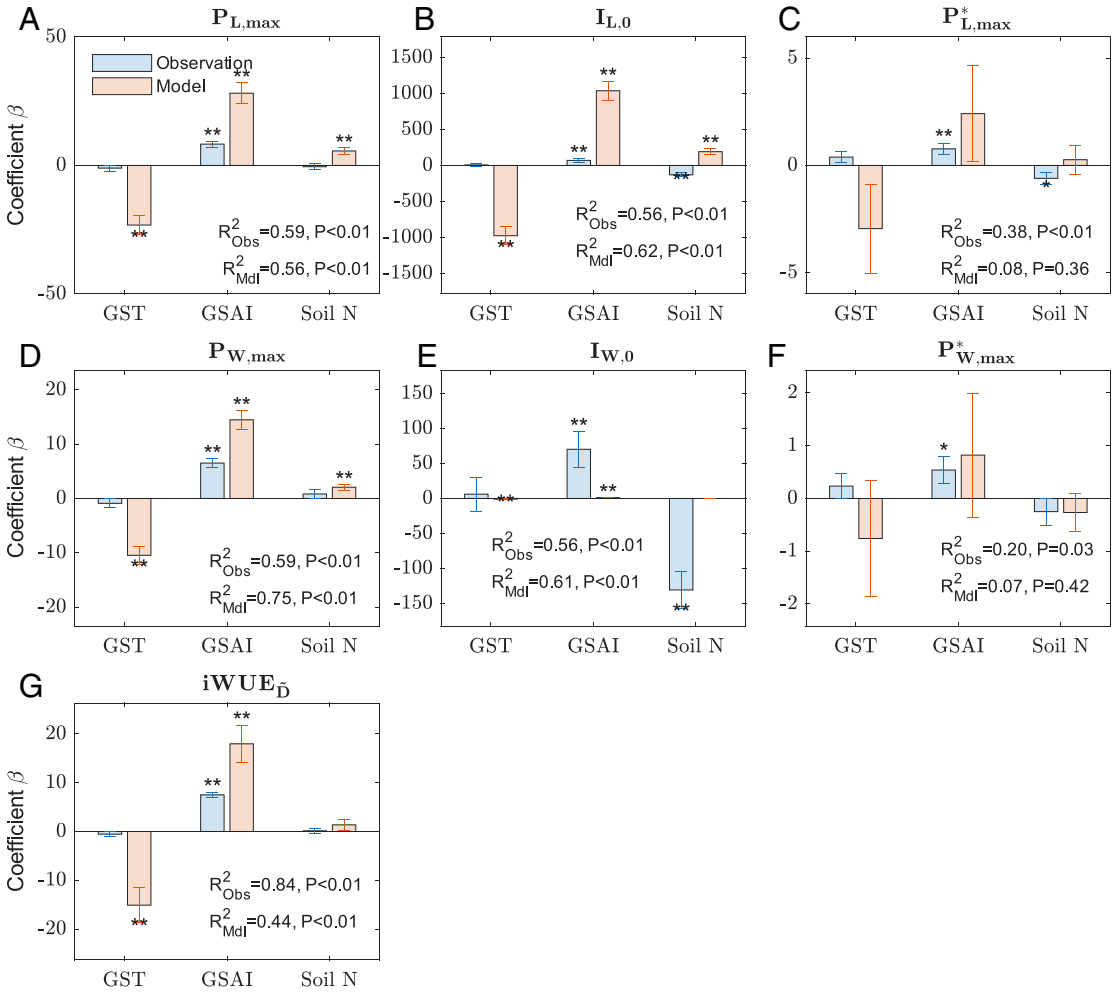


Fig. 3. The control of climate forcing on ecosystem process parameters: light use efficiency (LUE, top row, *A–C*), water use efficiency (WUE, middle row, *D–F*), and intrinsic water use efficiency ($iWUE_{\tilde{D}}$, bottom row, *G*). $P_{L,max}$ and $P_{W,max}$ are the maximum GPP given saturating light and full hydration, respectively; $I_{L,0}$ and $I_{W,0}$ are the half-saturation points of light and water use, respectively; $P^*_{L,max}$ and $P^*_{W,max}$ are $P_{L,max}$ and $P_{W,max}$ per unit leaf area. $iWUE_{\tilde{D}}$ is intrinsic water use efficiency at site-specific median vapor pressure deficit. GST is growing season mean temperature (°C), GSAI is growing season aridity index, and soil N is soil nitrogen concentration (g N/m^2 at top 1 m soil). The stars indicate the *t*-statistical significance of coefficient β, the whiskers are the SE of estimation (Eq. **4**), *P < 0.05 and **P < 0.01).

Discussion

Our approach showed strong control of forest ecosystem processes by plant functional traits across the continental USA. Supporting our first hypothesis, all three CWM plant functional traits—$\overline{V_{c,max}}$, $\overline{K_{l,max}}$ and $\overline{\pi_{tlp}}$—explained variation in ecosystem productivity and RUEs across diverse forests, with a mechanistic role supported by model simulations. The control of ecosystem productivity and RUEs by functional traits was similar to or stronger than that of climate variables (with respect to R^2 values, *SI Appendix*, Fig. S13), of which GSAI was the most important driver. We also found support for our second hypothesis: sites with higher $\overline{V_{c,max}}$ and $\overline{\pi_{tlp}}$ values had higher light- and water-saturated GPP and $iWUE_{\tilde{D}}$. This finding indicates that the concept of "acquisitive strategy," well established at the scale of plant species (48, 49), can be extended to whole ecosystems, based on their acquisitive CWM functional traits and moister climate, as has been theoretically suggested (18, 50). Further, consistent with our third hypothesis, sites with higher $\overline{V_{c,max}}$, representing an acquisitive strategy at ecosystem scale, showed greater sensitivity of LUE to SWC. In the observation dataset, our analysis did not resolve the effect of CWM functional trait values on the response of other ecosystem processes to SWC.

We discuss the mechanisms by which plant functional traits and climate regulate ecosystem processes, and propose explanations for the limited predictability of ecosystem-process sensitivity to SWC. We also discuss the importance of differentiating iWUE and WUE—commonly used indicators of water use strategy that show opposite responses to SWC changes at ecosystem scale (*SI Appendix*, *Text S5*). Finally, we consider potential reasons for the discrepancies between model simulations and observations in the predicted associations of ecosystem processes with CWM traits and climate, and we highlight avenues for improved modeling to predict forest responses to shifts in climate and species distributions (*SI Appendix*, *Text S6*).

Mechanisms of Plant Trait Controls on Ecosystem Functions. All three plant functional traits in our analysis were expected to have strong influences on ecosystems across the continental gradient. Thus, the positive correlations of light- and water-saturated GPP and $iWUE_{\tilde{D}}$ with $\overline{V_{c,max}}$ (Fig. 2) would follow from the direct scaling up of leaf physiology to ecosystem processes at a continental scale. $V_{c,max}$ is influenced primarily

Downloaded from https://www.pnas.org by HARVARD UNIVERSITY; CABOT SCIENCE LIBRARY on November 19, 2026 from IP address 140.247.220.94.

by the concentration of Rubisco in the leaf, which determines maximum rates of CO_2 fixation (51). Therefore, under the same environmental conditions, ecosystems with higher $\overline{V_{c,max}}$ would be expected to assimilate more carbon and show higher RUEs (19, 52). Similarly, leaf hydraulic conductance is an important determinant of plant water use and gas exchange, given that leaves are a hydraulic bottleneck within the plant (42). Across species, stomatal conductance and maximum leaf photosynthetic capacity are related to $K_{l,max}$ (22, 23). This trend scales up to the whole ecosystem, such that higher $\overline{K_{l,max}}$ would contribute to higher productivity and lower iWUE and WUE, though the trend for WUE was only found in the observed dataset and not the model simulation (Figs. 2 and 3) (52, 53). Finally, π_{tlp} is a trait that confers drought tolerance at leaf and plant scales, and across species (25); a higher π_{tlp} is related to a higher stomatal conductance at the leaf scale (26). This pattern, when scaled up to the ecosystem, explains the positive correlation of ecosystem process parameters with $\overline{\pi_{tlp}}$.

Mechanisms of Climate Controls on Ecosystem Processes. Our results also show strong control by climate drivers over multiple ecosystem process parameters. Notably, our hierarchical partitioning analyses supported an independent role for CWM traits in driving variation in productivity and RUEs across forests, with CWM traits explaining a similar share of R^2 as climate variables across ecosystem process parameters (*SI Appendix*, Fig. S13). Yet, CWM functional traits were partially interrelated with climate, with combined influences on ecosystem processes. Among the three environmental factors, GSAI had the strongest influence on the measured ecosystem processes. Notably, ecosystems in moister climates tended to show an acquisitive strategy, including a high $\overline{\pi_{tlp}}$ (27) (*SI Appendix*, Fig. S12), which would drive increased LUE, WUE, and $iWUE_{\tilde{D}}$ via its association with high light- and water-saturated GPP (Fig. 2). In addition, we found higher $\overline{V_{c,max}}$ values in wetter sites. Multiple studies have reported that drought suppresses ecosystem productivity and LUE, especially during the peak growing season, partly as a consequence of reduced $V_{c,max}$—under strong water stress, this can also lead to decreased WUE (7, 54–56). Thus, the association of this functional trait with climate would contribute to the positive correlation between ecosystem process parameters and GSAI (*SI Appendix*, Fig. S12). Additionally, the influence of GST on ecosystem processes at continental scale may be in part mediated by $V_{c,max}$. Temperature controls the enzyme kinetics that determine $V_{c,max}$ and other metabolic activities (57), with nonlinear effects, where enzyme activity rises under warmer conditions and declines under severe heat stress (58).

We also found that soil N was a driver of ecosystem processes. Indeed, previous studies found that Rubisco concentration and photosynthetic rates are positively associated with higher leaf N (59–61). Additionally, higher N availability may enable higher $K_{l,max}$ and π_{tlp} by promoting vessel enlargement and the availability of photosynthate to allocate to osmotic adjustment (62). However, the observation dataset did not support these relationships: light- and water-saturated GPP showed no significant relationship with soil N, and GPP normalized by LAI was negatively related to N. The inconsistency between the observations and the literature may stem from the coarse resolution of the global soil N dataset used (63), which does not capture the coupling between soil and leaf N concentrations. Modeled light- and water-saturated GPP did increase with N availability, consistent with the literature. This apparent agreement, however, is not mechanistic, because LM4.1 does not represent the nitrogen cycle, and likely reflects indirect correlations rather than causal processes.

Weak Control of Plant Functional Traits and Climate Forcing on Ecosystem Processes' Sensitivity to Soil Moisture. Our analysis examined the influence of CWM plant functional traits on the sensitivity of ecosystem processes to SWC. For example, the observed sensitivity of $P_{L,max}$ to SWC was positively related to $\overline{V_{c,max}}$, and the sensitivity of modeled $P^*_{L,max}$ to SWC was positively related to $\overline{K_{l,max}}$. These patterns supported our third hypothesis that ecosystems assembled in wetter environments have developed an acquisitive strategy and would be more susceptible to drought events. Yet, most of the relationships we tested between functional traits or climate variables and ecosystem-process sensitivity to SWC were not statistically significant. A lack of such associations may partly stem from interspecific variability in plants' responses to water stress. While CWM functional traits effectively explain site-level differences in ecosystem processes, the sensitivity of these processes to SWC may be driven by species-specific responses not captured by CWM canopy traits (12, 18).

Limitations and Future Work. Our analyses provide evidence for the critical role of leaf photosynthetic and hydraulic traits for shaping ecosystem responses to environmental stressors. Further, this work demonstrates the ability of Vegetation Dynamic Models, informed by CWM functional traits, to reproduce these responses. Previous studies at individual sites have shown that annual GPP can be well predicted by the product of leaf $V_{c,max}$ and LAI (64). Our approach extends this $V_{c,max} \times LAI$ framework by a) using the CWM value of $\overline{V_{c,max}}$ to incorporate which species dominate each forest (65); b) decomposing GPP into light- and water-saturated components to reveal the specific pathways through which traits control productivity; and c) adding $\overline{K_{l,max}}$ and $\overline{\pi_{tlp}}$ to capture across-ecosystem variation in water transport and drought tolerance, dimensions absent from the $V_{c,max} \times LAI$ framework.

The limitations of the model could account for several discrepancies between simulated and observed associations of functional traits with ecosystem processes, such as the effect of $\overline{K_{l,max}}$ on $iWUE_{\tilde{D}}$. Notably, the model represents the ecosystem as a single species with CWM functional traits (18), an approach we adopted given current limitations in parameterizing models with multiple coexisting species or PFTs (66). However, plant species have different responses to environmental drivers, and interactions among species, such as complementarity and competition, might generate outcomes that deviate from expected average behavior. For example, the species-level trade-off between hydraulic efficiency and safety may be weakened at the ecosystem scale by biodiversity (67), and thus cannot be captured by models representing each ecosystem as a single species with CWM trait values. Additionally, neither the model nor the use of CWM traits resolves the influences of species size-distributions, intraspecific trait variation, or temporal trait variation. For example, $V_{c,max}$ varies seasonally with leaf age and along the canopy profile (64). Further, the model did not include the possibility of interactive effects among functional traits and climate sensitivity (*SI Appendix*, *Text S6*). Future work is needed to improve the representation of species functional diversity in Vegetation Dynamic Models (68, 69) to explore the role of diversity in ecosystem processes such as productivity, RUEs, and their responses to drought (70). We emphasize the ongoing need to improve models by appropriately representing functional traits and their roles in driving ecosystem processes, and by calibrating against measured traits across ecosystems.

Downloaded from https://www.pnas.org by HARVARD UNIVERSITY; CABOT SCIENCE LIBRARY on November 19, 2026 from IP address 140.247.220.94.

Conclusions. We found that CWM plant functional traits ($\overline{V_{c,max}}$, $\overline{K_{l,max}}$ and $\overline{\pi_{tlp}}$) have influences similar to or stronger than those of climate on temperate forests' productivity and RUEs across the continental USA. These findings were generally supported by model simulations, validating a mechanistic basis. We found that forests with higher CWM $\overline{V_{c,max}}$ and $\overline{\pi_{tlp}}$ and wetter climates showed an overall greater acquisitive strategy at the ecosystem level, with higher light- and water-saturated GPP and $iWUE_{\tilde{D}}$. Among climate variables, GSAI was the strongest driver of ecosystem processes. We resolved only limited influence of CWM traits on the response of ecosystem processes to SWC, which suggests that inter- and intraspecific variability in responses to water stress is a key avenue for understanding the sensitivity of ecosystem processes to drought.

Methods

Study Sites. Eight deciduous- and conifer-dominated forests across the United States were selected to span broad temperature and moisture gradients. All eight forests are NEON or AmeriFlux sites with continuous multiple-year flux measurements (Fig. 1 and Table 1). For each site, we restricted our analyses to the years with the most complete peak-growing-season records of carbon flux, water flux, and soil water content (SWC). At HARV, OSBS, GRSM, PFS, NR1, and SJER, where Broadleaf-Deciduous and Conifer-Evergreen species coexist, we represented each forest by its dominant leaf form and habit for modeling purposes.

Ecosystem Processes. We determined the light use efficiency (LUE), water use efficiency (WUE), and intrinsic water use efficiency (iWUE) during the peak growing season as

$$LUE = \frac{GPP}{I}, \quad [1a]$$

$$WUE = \frac{GPP}{ET}, \quad [1b]$$

$$iWUE = \frac{GPP}{G_c}, \quad [1c]$$

where GPP is gross primary productivity, i.e., the CO_2 assimilation rate (μmol C m^{-2} s^{-1}), I is the photosynthetic photon flux density (μmol photon m^{-2} s^{-1}), ET is the evapotranspiration (mmol H_2O m^{-2} s^{-1}), and G_c is the canopy conductance (mol H_2O m^{-2} s^{-1}; for computation see *SI Appendix*, *Text S7*).

LUE is the amount of CO_2 assimilated (GPP) per unit irradiance. A rectangular hyperbolic equation often describes the relationship between GPP and I (6):

$$GPP(I) = \frac{P_{L,max} \times I}{I + I_{L,0}}, \quad [2]$$

where $P_{L,max}$ is the maximum GPP as $I \to \infty$ and $I_{L,0}$ represents the light level corresponding to the half-saturation point, i.e., $GPP(I_{L,0}) = \frac{P_{L,max}}{2}$. A lower $I_{L,0}$ value indicates GPP saturates at relatively low I, thereby being more responsive under light-limited conditions.

WUE describes the amount of carbon fixed per unit of water evaporated. We replaced I in Eq. **2** with evapotranspiration (ET, mmol H_2O m^{-2} s^{-1}), and replaced the symbol $P_{L,max}$ by $P_{W,max}$ for maximum GPP given sufficient water; we also replaced $I_{L,0}$ by $I_{W,0}$ to describe the half-saturation point where $GPP(I_{W,0}) = \frac{P_{W,max}}{2}$. An example showing how $P_{W,max}$ and $I_{W,0}$ control the GPP water-response curve, and how $P_{L,max}$ and $I_{L,0}$ control the GPP light-response curve, is presented in *SI Appendix*, Fig. S14.

Notably, ET is directly driven by vapor pressure deficit (D), and thus WUE tends to decline with increasing D. By contrast, iWUE tends to increase at higher D, due to stomatal closure (71). We used a linear function of D to model leaf-level response [e.g., Leuning (72)] to capture its variability, i.e.,

$$iWUE(D) = \frac{GPP}{G_c} = \frac{C_a - \Gamma^*}{m} + \frac{C_a - \Gamma^*}{m}\frac{D}{D_0} = a + bD, \quad [3]$$

where C_a is the ambient CO_2 concentration, Γ^* is the CO_2 compensation point, and m [equivalent to a_1 in Leuning (72)] and D_0 are fitted parameters. By fitting (Eqs. **2** and **3**), we obtained parameters describing these ecosystem processes–hereafter referred to as "ecosystem process parameters" (Table 2). Additionally, we normalized $P_{L,max}$ and $P_{W,max}$ by LAI to interpret these ecosystem process parameters per unit of leaf area (indicated as $P^*_{L,max}$ and $P^*_{W,max}$). For the observation-derived ecosystem process parameters, we used MODIS LAI. For the model-derived ecosystem process parameters, we used the simulated LAI. For *iWUE*, we evaluated its value at the site-specific median of D (i.e., D~) during daytime in the growing season. Examples of fitted ecosystem processes are shown in *SI Appendix*, Fig. S15.

Field Measurements. The plant functional traits analyzed in this study were the maximum rate of carboxylation ($V_{c,max}$, μmol m^{-2} s^{-1}), maximum leaf hydraulic conductance ($K_{l,max}$, mmol m^{-2} s^{-1} MPa^{-1}), and turgor loss point (π_{tlp}, MPa). These functional traits were measured for the most abundant species at each site, which together accounted for >90% of basal area based on the available forest inventory data. For each site, the CWM functional traits were computed as a weighted average using species above-ground biomass. Because $K_{l,max}$ measurements were not available for SERC, we substituted values from a nearby, highly similar site, the Smithsonian Conservation Biology Institute (SCBI). The technical details of the design, biomass estimation, and functional trait measurements are provided in *SI Appendix*, *Text S8*. Across the eight forests, we observed a wide variation in trait values (*SI Appendix*, Fig. S16) corresponding to the diverse resource use strategies of the different ecosystems.

Flux tower data used to compute the ecosystem processes (Eqs. **1**–**3**) were obtained from the AmeriFlux database (https://ameriflux.lbl.gov). A constant multiplier was applied to sensible heat (H) and latent heat (LE) to address the surface energy imbalance between H+LE and available energy (73). GPP was partitioned from net ecosystem exchange (NEE) using a custom function based on the light-response curve, which avoids relying on nighttime fluxes (8).

Model Simulation and Sensitivity Analysis. The model used in this study is the terrestrial component of Geophysical Fluid Dynamics Laboratory's (GFDL) Earth System Model Version 4.1 (ESM4.1) - Land Model 4.1 (LM4.1). A detailed description and the list of equations on the model's photosynthesis and plant hydraulics processes is in *SI Appendix*, *Text S2*. LM4.1 uses $V_{c,max}$ and $K_{l,max}$ as species-level input parameters. In this study, we represented each forest as a single composite species parameterized with the measured CWM trait values ($\overline{V_{c,max}}$ and $\overline{K_{l,max}}$). Based on the typical correspondence of π_{tlp} to the threshold for half-stomatal closure (74), we used the measured $\overline{\pi_{tlp}}$ to derive the model parameter that controls the decline of photosynthetic rate with water stress (d_l in *SI Appendix*, Eqs. **S4** and **S5**). The dark respiration parameter γ_{res} (*SI Appendix*, Eq. **S1b**) and water use efficiency parameter m (*SI Appendix*, Eq. **S3**) were calibrated against the measured ecosystem functions with Parallel Optimization with Dynamic coordinate search using Surrogates (PODS) (*SI Appendix*, *Text S3*) (75).

After calibration, the sensitivity of the modeled ecosystem process parameters (Table 2) to $\overline{V_{c,max}}$, $\overline{K_{l,max}}$, $\overline{\pi_{tlp}}$, GST, and GSP was tested for each of the eight ecosystems (*SI Appendix*, *Text S4*).

Fitting Ecosystem Process and Evaluation of its Control by Plant Functional Traits and Climate. The controls of plant functional traits and climate forcing on ecosystem processes were analyzed by fitting a linear regression model:

$$y_i = \beta_0 + \beta_1 x_{1,i} + \beta_2 x_{2,i} + \beta_3 x_{3,i} + \varepsilon_i \quad [4]$$

where y_i is an ecosystem process parameter for site i (Table 2), and $x_{1,i}$, $x_{2,i}$ and $x_{3,i}$ are $\overline{V_{c,max}}$, $\overline{K_{l,max}}$, and $\overline{\pi_{tlp}}$ when analyzing plant functional trait control, and growing season temperature (GST), growing season aridity index [GSAI; ratio between growing season precipitation (GSP, mm) and growing season potential evapotranspiration (GSPET, mm) (76)], and soil N content in the top 1 m (gN m^{-2}) when analyzing climatic controls (63). GST and GSP were computed from model forcing and flux tower measurements for the modeled and observation datasets, respectively. GSPET was calculated using the Penman equation (77). The comparison of modeled and observed forcing is given in *SI Appendix*, Fig. S17. The growing season period for each site is given in *SI Appendix*, Table S1. We also tested the control of annual, spring, summer, fall, and winter temperature, as well as aridity index (AI, as precipitation/potential evapotranspiration) on ecosystem processes, and found that growing season variables were more powerful

Downloaded from https://www.pnas.org by HARVARD UNIVERSITY; CABOT SCIENCE LIBRARY on November 19, 2026 from IP address 140.247.220.94.

for resolving environmental influences. The coefficients β of annual and seasonal control over ecosystem processes are provided in Dataset S1. We also tested the relative importance of each trait and climate forcing variable in explaining ecosystem process parameters by fitting all six factors into one linear equation and computing their hierarchical partition of R^2. To differentiate from ecosystem process parameters, the fitting parameters in Eq. **4** are referred to as "coefficients."

The Sensitivity of Ecosystem Functions to Soil Water Stress. We tested how ecosystem functions respond to soil water stress, and how plant functional traits and climate forcing modulate those responses, by dividing the growing season soil moisture into five quantiles (*SI Appendix*, Fig. S18). We fitted ecosystem processes for each quantile with a mixed-effects model to estimate the ecosystem sensitivity to soil water stress:

$$\begin{cases} y_{i,j} = \beta_{0,i} + \beta_{1,i} \times SWC_{i,j} + \varepsilon_{i,j} \\ \beta_{0,i} = a_0 + \eta_{0,i} \\ \beta_{1,i} = a_1 + \eta_{1,i} \end{cases} \quad [5]$$

where $y_{i,j}$ is the process parameter for forest i for SWC quantile j. In Eq. **5**, a_0 and a_1 are fixed effects of intercept and slope, while $\eta_{0,i}$ and $\eta_{1,i}$ are site-specific random effects. Upon identifying a significant impact of SWC on ecosystem process parameters (i.e., significance of $\beta_{1,i}$, *SI Appendix*, *Text S9*), we analyzed the influence of plant functional traits on this sensitivity by modeling $\beta_{0,i}$ and $\beta_{1,i}$ as functions of x_i (i.e., $\overline{V_{c,max}}$, $\overline{K_{l,max}}$, $\overline{\pi_{tlp}}$, GST, GSAI, or soil N concentration):

$$\begin{cases} \beta_{0,i} = a_0 + b_0 x_i + \eta_{0,i} \\ \beta_{1,i} = a_1 + b_1 x_i + \eta_{1,i} \end{cases} \quad [6]$$

where b_0 and b_1 represent the dependence of the intercept and slope on x. In particular, b_1 indicates the control of x over β_1, thereby indicating how plant functional traits or climate factors influence the sensitivity of ecosystem processes to SWC. A positive b_1 indicates that sites with a higher value of the trait x are more sensitive to SWC. Consistent with the previous section, all parameters in Eqs. **5** and **6** are referred to as "coefficients." All coefficients were estimated using MATLAB's fit linear mixed-effects model function. All predictors x were normalized as z-scores before analysis.

Data, Materials, and Software Availability. All data and code supporting this study are publicly available in the Zenodo repository (78). All other data are included in the article and/or supporting information.

ACKNOWLEDGMENTS. This study was supported by NSF Grant 2017804. We thank Jennifer Franklin, Audrey Barker Plotkin, Stephanie Bohlman, Nicolas Tarasewicz, N. Michele Holbrook, Geoffrey Parker, Grace John, Kenneth Clark, and Jeffrey Warren for assistance in field operations. K.C.C. was supported by the Laboratory Directed Research and Development Program of Oak Ridge National Laboratory (ORNL); ORNL is managed by the University of Tennessee-Battelle, limited liability company, under contract DE-AC05-00OR22725 with the U.S. Department of Energy.

Author affiliations: [a]High Meadows Environmental Institute, Princeton University, Princeton, NJ 08544; [b]Department of Ecology and Evolutionary Biology, University of California, Los Angeles, CA 90095-1606; [c]Virginia Tech, Department of Forest Resources and Environmental Conservation, Virginia Polytechnic Institute and State University, VA 24061; [d]Department of Botany, Federal University of Pernambuco, Biosciences Center, Recife, Pernambuco 50670-901, Brazil; [e]Department of Earth System Sciences, Stanford University, Stanford, CA 94305; [f]School of Natural Resources, University of Missouri, Columbia, MO 65211; [g]Division of Environmental Sciences, Oak Ridge National Laboratory, Oak Ridge, TN 37830; [h]National Oceanic and Atmospheric Administration Geophysical Fluid Dynamics Laboratory, Princeton, NJ 08540; [i]Department of Geography, University of California Santa Barbara, Santa Barbara, CA 93106; [j]Harvard Forest, Harvard University, Petersham, MA 01366; [k]Massachusetts Department of Conservation and Recreation, Boston, MA 02116; [l]School of the Environment, Yale University, New Haven, CT 06511; [m]School of Forest, Fisheries, and Geomatics Sciences, University of Florida, Gainesville, FL 32611; [n]School of Renewable Natural Resources, Louisiana State University, Baton Rouge, LA 70803; [o]Smithsonian Environmental Research Center, Edgewater, MD 21037; [p]Amap Lab, University of Montpellier, Ird, Cirad, Cnrs, Inrae, Montpellier 34394, France; [q]Department of Earth and Environmental Sciences, Rutgers University, Newark, NJ 07102; [r]Department of Geography, University of Colorado, Boulder, CO 80309-0260; [s]National Science Foundation National Center for Atmospheric Research, Boulder, CO 80301; and [t]Civil and Environmental Engineering, Princeton University, Princeton, NJ 08544

1. B. D. Stocker *et al.*, Drought impacts on terrestrial primary production underestimated by satellite monitoring. *Nat. Geosci.* **12**, 264–270 (2019).
2. T. J. Brodribb, J. Powers, H. Cochard, B. Choat, Hanging by a thread? Forests and drought. *Science* **368**, 261–266 (2020).
3. D. L. Miller *et al.*, Increased photosynthesis during spring drought in energy-limited ecosystems. *Nat. Commun.* **14**, 7828 (2023).
4. H. Yang *et al.*, Global increase in biomass carbon stock dominated by growth of northern young forests over past decade. *Nat. Geosci.* **16**, 886–892 (2023).
5. National Academies of Sciences, *Engineering, and Medicine, A Vision for Continental-Scale Biology: Research Across Multiple Scales* (The National Academies Press, Washington, DC, (2025). p. 176.
6. A. Ruimy, P. G. Jarvis, D. D. Baldocchi, B. Saugier, "CO2 fluxes over plant canopies and solar radiation: A review" in *Advances in Ecological Research*, M. Begon, A. H. Fitter, Eds. (Academic Press, 1995), vol. 26, pp. 1–68.
7. M. Reichstein *et al.*, Severe drought effects on ecosystem CO_2 and H_2O fluxes at three Mediterranean evergreen sites: Revision of current hypotheses? *Glob. Chang. Biol.* **8**, 999–1017 (2002).
8. M. Detto, S. W. Pacala, Plant hydraulics, stomatal control, and the response of a tropical forest to water stress over multiple temporal scales. *Glob. Chang. Biol.* **28**, 4359–4376 (2022).
9. M. Migliavacca *et al.*, The three major axes of terrestrial ecosystem function. *Nature* **598**, 468–472 (2021).
10. M. F. Garbulsky *et al.*, Patterns and controls of the variability of radiation use efficiency and primary productivity across terrestrial ecosystems. *Glob. Ecol. Biogeogr.* **19**, 253–267 (2010).
11. Y. Yang *et al.*, Contrasting responses of water use efficiency to drought across global terrestrial ecosystems. *Sci. Rep.* 6, 23284 (2016).
12. M. Reichstein, M. Bahn, M. D. Mahecha, J. Kattge, D. D. Baldocchi, Linking plant and ecosystem functional biogeography. *Proc. Natl. Acad. Sci. U.S.A.* **111**, 13697–13702 (2014).
13. S. Lavorel, E. Garnier, Predicting changes in community composition and ecosystem functioning from plant traits: Revisiting the holy grail. *Funct. Ecol.* **16**, 545–556 (2002).
14. C. Violle *et al.*, Let the concept of trait be functional! *Oikos* **116**, 882–892 (2007).
15. B. J. McGill, B. J. Enquist, E. Weiher, M. Westoby, Rebuilding community ecology from functional traits. *Trends Ecol. Evol.* **21**, 178–185 (2006).
16. Y. Cao, X. Feng, L.-H. Lin, N. Wei, J. Tan, Revisiting competitive outcomes through a trait lens: A global meta-analysis across species provenance. *Nat. Commun.* **16**, 10639 (2025).
17. R. Muscarella, M. Uriarte, Do community-weighted mean functional traits reflect optimal strategies? *Proc. R. Soc. Lond. B. Biol. Sci.* **283**, 20152434 (2016).
18. J. D. Wood *et al.*, The ecosystem as super-organ/ism, revisited: Scaling hydraulics to forests under climate change. *Integr. Comp. Biol.* **64**, 424–440 (2024).
19. E. Carmo-Silva, J. C. Scales, P. J. Madgwick, M. A. J. Parry, Optimizing Rubisco and its regulation for greater resource use efficiency. *Plant Cell Environ.* **38**, 1817–1832 (2015).
20. L. Sack, N. Holbrook, Leaf hydraulics. *Annu. Rev. Plant Biol.* **57**, 361–381 (2006).
21. S. C. Wong, I. R. Cowan, G. D. Farquhar, Stomatal conductance correlates with photosynthetic capacity. *Nature* **282**, 424–426 (1979).
22. T. J. Brodribb, T. S. Feild, G. J. Jordan, Leaf maximum photosynthetic rate and venation are linked by hydraulics. *Plant Physiol.* **144**, 1890–1898 (2007).
23. C. Scoffoni *et al.*, Hydraulic basis for the evolution of photosynthetic productivity. *Nat. Plants* **2**, 16072 (2016).
24. M. Ye, M. Wu, H. Zhang, Z. Zhang, Z. Zhang, High leaf vein density promotes leaf gas exchange by enhancing leaf hydraulic conductance in Oryza sativa L. *Plants Front. Plant Sci* **12**, 693815 (2021).
25. M. K. Bartlett, C. Scoffoni, L. Sack, The determinants of leaf turgor loss point and prediction of drought tolerance of species and biomes: A global meta-analysis. *Ecol. Lett.* **15**, 393–405 (2012).
26. C. Henry *et al.*, A stomatal safety-efficiency trade-off constrains responses to leaf dehydration. *Nat. Commun.* **10**, 3398 (2019).
27. S.-D. Zhu *et al.*, Leaf turgor loss point is correlated with drought tolerance and leaf carbon economics traits. *Tree Physiol.* **38**, 658–663 (2018).
28. Y. Jin *et al.*, Precipitation, solar radiation, and their interaction modify leaf hydraulic efficiency–safety trade-off across angiosperms at the global scale. *New Phytol.* **244**, 2267–2277 (2024).
29. J. Bota, H. Medrano, J. Flexas, Is photosynthesis limited by decreased Rubisco activity and RuBP content under progressive water stress? *New Phytol.* **162**, 671–681 (2004).
30. J. Kumar, W. W. Hargrove Jr., S. P. Norman, F. M. Hoffman, D. Newcomb, "Characterization and classification of vegetation canopy structure and distribution within the Great Smoky Mountains National Park using LiDAR" in *Proceedings 15th IEEE International Conference on Data Mining Workshop* (IEEE, Atlantic City, NJ, USA, 2015) pp. 8.
31. K. L. Clark, C. Aoki, M. Ayres, J. Kabrick, M. R. Gallagher, Insect infestations and the persistence and functioning of oak-pine mixedwood forests in the mid-Atlantic region, USA. *PLoS One* **17**, e0265955 (2022).
32. L. Gu *et al.*, Testing a land model in ecosystem functional space via a comparison of observed and modeled ecosystem flux responses to precipitation regimes and associated stresses in a central U.S. forest. *J. Geophys. Res. Biogeosci.* **121**, 1884–1902 (2016).
33. H. J. Renninger, N. Carlo, K. L. Clark, K. V. R. Schäfer, Physiological strategies of co-occurring oaks in a water- and nutrient-limited ecosystem. *Tree Physiol.* **34**, 159–173 (2014).
34. Y. Li, Climate feedback from plant physiological responses to increasing atmospheric CO_2 in Earth system models. *New Phytol.* **244**, 2176–2182 (2024).
35. B. F. Rius *et al.*, Higher functional diversity improves modeling of Amazon forest carbon storage. *Ecol. Model.* **481**, 110323 (2023).
36. E. Weng, C. E. Farrior, R. Dybzinski, S. W. Pacala, Predicting vegetation type through physiological and environmental interactions with leaf traits: Evergreen and deciduous forests in an earth system modeling framework. *Glob. Chang. Biol.* **23**, 2482–2498 (2017).
37. A. Rogers, The use and misuse of Vc, max in Earth system models. *Photosynth. Res.* **119**, 15–29 (2014).
38. N. G. McDowell, T. J. Brodribb, A. Nardini, Hydraulics in the 21st century. *New Phytol.* **224**, 537–542 (2019).
39. J. M. Torres-Ruiz *et al.*, Plant hydraulics at the heart of plant, crops and ecosystem functions in the face of climate change. *New Phytol.* **241**, 984–999 (2024).

Downloaded from https://www.pnas.org by HARVARD UNIVERSITY; CABOT SCIENCE LIBRARY on November 19, 2026 from IP address 140.247.220.94.

40. B. O. Christoffersen *et al.*, Linking hydraulic traits to tropical forest function in a size-structured and trait-driven model (TFS vol 1-Hydro). *Geosci. Model Dev.* **9**, 4227–4255 (2016).
41. E. Shevliakova *et al.*, The land component LM4.1 of the GFDL earth system model ESM4.1: Model description and characteristics of land surface climate and carbon cycling in the historical simulation. *J. Adv. Model. Earth Syst.* **16**, e2023MS003922 (2024).
42. B. T. Wolfe *et al.*, Leaves as bottlenecks: The contribution of tree leaves to hydraulic resistance within the soil−plant−atmosphere continuum. *Plant Cell Environ.* **46**, 736–746 (2023).
43. L. M. Verheijen *et al.*, Impacts of trait variation through observed trait–climate relationships on performance of an Earth system model: A conceptual analysis. *Biogeosciences* **10**, 5497–5515 (2013).
44. S. Bao *et al.*, Toward robust parameterizations in ecosystem-level photosynthesis models. *J. Adv. Model. Earth Syst.* **15**, e2022MS003464 (2023).
45. G.-Q. Yao *et al.*, Combined high leaf hydraulic safety and efficiency provides drought tolerance in *Caragana* species adapted to low mean annual precipitation. *New Phytol.* **229**, 230–244 (2021).
46. Y. Malhi *et al.*, The variation of productivity and its allocation along a tropical elevation gradient: A whole carbon budget perspective. *New Phytol.* **214**, 1019–1032 (2017).
47. M.-M. Holloway-Phillips, T. J. Brodribb, Minimum hydraulic safety leads to maximum water-use efficiency in a forage grass. *Plant Cell Environ.* **34**, 302–313 (2011).
48. J. P. Grime, *Plant Strategies, Vegetation Processes, and Ecosystem Properties* (John Wiley & Sons, Chichester, United Kingdom, ed. 2, 2001).
49. P. B. Reich, The world-wide "fast–slow" plant economics spectrum: A traits manifesto. *J. Ecol.* **102**, 275–301 (2014).
50. U. Gomarasca *et al.*, Leaf-level coordination principles propagate to the ecosystem scale. *Nat. Commun.* **14**, 3948 (2023).
51. J. Galmés *et al.*, Rubisco specificity factor tends to be larger in plant species from drier habitats and in species with persistent leaves. *Plant Cell Environ.* **28**, 571–579 (2005).
52. J. Flexas *et al.*, Mesophyll conductance to CO_2 and Rubisco as targets for improving intrinsic water use efficiency in C3 plants. *Plant Cell Environ.* **39**, 965–982 (2016).
53. A. Nardini, J. Luglio, Leaf hydraulic capacity and drought vulnerability: Possible trade-offs and correlations with climate across three major biomes. *Funct. Ecol.* **28**, 810–818 (2014).
54. M. Reichstein *et al.*, Reduction of ecosystem productivity and respiration during the European summer 2003 climate anomaly: A joint flux tower, remote sensing and modelling analysis. *Glob. Chang. Biol.* **13**, 634–651 (2007).
55. J. Ma *et al.*, Ecosystem water use efficiency in a young plantation in Northern China and its relationship to drought. *Agric. For. Meteorol.* **275**, 1–10 (2019).
56. F. Zhang *et al.*, How recent climate change influences water use efficiency in East Asia. *Theor. Appl. Climatol.* **116**, 359–370 (2014).
57. Z. Yan *et al.*, Global patterns and drivers of leaf photosynthetic capacity: The relative importance of environmental factors and evolutionary history. *Glob. Ecol. Biogeogr.* **32**, 668–682 (2023).
58. J. Galmés, I. Aranjuelo, H. Medrano, J. Flexas, Variation in Rubisco content and activity under variable climatic factors. *Photosynth. Res.* **117**, 73–90 (2013).
59. X. Mu, Y. Chen, The physiological response of photosynthesis to nitrogen deficiency. *Plant Physiol. Biochem.* **158**, 76–82 (2021).
60. J. R. Evans, Photosynthesis and nitrogen relationships in leaves of C3 plants. *Oecologia* **78**, 9–19 (1989).
61. X. Liang *et al.*, Global response patterns of plant photosynthesis to nitrogen addition: A meta-analysis. *Glob. Chang. Biol.* **26**, 3585–3600 (2020).
62. T. Zhang *et al.*, Leaf hydraulic acclimation to nitrogen addition of two dominant tree species in a subtropical forest. *Sci. Total Environ.* **771**, 145415 (2021).
63. Global-Soil-Data-Task-Group, Global gridded surfaces of selected soil characteristics (IGBP-DIS). https://doi.org/10.3334/ORNLDAAC/569 (2000) Accessed 1 September 2024.
64. R. Wang, J. M. Chen, X. Luo, A. Black, A. Arain, Seasonality of leaf area index and photosynthetic capacity for better estimation of carbon and water fluxes in evergreen conifer forests. *Agric. For. Meteorol.* **279**, 107708 (2019).
65. N. He *et al.*, Predicting ecosystem productivity based on plant community traits. *Trends Plant Sci.* **28**, 43–53 (2023).
66. Y. Cheng, W. Wang, M. Detto, R. Fisher, C. Shoemaker, Calibrating tropical forest coexistence in ecosystem demography models using multi-objective optimization through population-based parallel surrogate search. *J. Adv. Model. Earth Syst.* **16**, e2023MS004195 (2024).
67. W. R. L. Anderegg, J. Martinez-Vilalta, M. Mencuccini, R. Poyatos, Community assembly influences plant trait economic spectra and functional trade-offs at ecosystem scales. *Proc. Natl. Acad. Sci. U.S.A.* **121**, e2404034121 (2024).
68. R. A. Fisher *et al.*, Vegetation demographics in Earth system models: A review of progress and priorities. *Glob. Chang. Biol.* **24**, 35–54 (2018).
69. M. Detto, X. Xu, Optimal leaf life strategies determine Vc, max dynamic during ontogeny. *New Phytol.* **228**, 361–375 (2020).
70. Y. Liu, Scaling plant hydraulic traits to predict ecosystem fluxes under drought. *New Phytol.* **250**, 2078–2084 (2026).
71. K. Yi *et al.*, Responses of marginal and intrinsic water-use efficiency to changing aridity using FLUXNET observations. *J. Geophys. Res. Biogeosci.* **129**, e2023JG007875 (2024).
72. R. Leuning, A critical appraisal of a combined stomatal-photosynthesis model for C3 plants. *Plant Cell Environ.* **18**, 339–355 (1995).
73. K. Wilson *et al.*, Energy balance closure at FLUXNET sites. *Agric. For. Meteorol.* **113**, 223–243 (2002).
74. M. K. Bartlett, T. Klein, S. Jansen, B. Choat, L. Sack, The correlations and sequence of plant stomatal, hydraulic, and wilting responses to drought. *Proc. Natl. Acad. Sci. U.S.A.* 113, 13098–13103 (2016).
75. W. Xia, C. Shoemaker, GOPS: Efficient RBF surrogate global optimization algorithm with high dimensions and many parallel processors including application to multimodal water quality PDE model calibration. *Optim. Eng.* **22**, 2741–2777 (2021).
76. C. J. Barrow, "Land degradation and development" in *Book Review: World Atlas of Desertification*, N. Middleton, D. S. G. Thomas, Eds. (United Nations Environment Programme, 1992).
77. H. L. Penman, Natural evaporation from open water, bare soil and grass. *Proc. R. Soc. Lond. A Math. Phys. Sci.* 193, 120–145 (1948).
78. B. Zhao *et al.*, Leaf hydraulic and photosynthetic traits mediate forest-scale resource use efficiencies across the continental USA. Zenodo. https://zenodo.org/records/23327763. Deposited 13 October 2026.

Downloaded from https://www.pnas.org by HARVARD UNIVERSITY; CABOT SCIENCE LIBRARY on November 19, 2026 from IP address 140.247.220.94.